Coordination of Fc receptor signaling regulates cellular commitment to phagocytosis

Youxin Zhang[a], Adam D. Hoppe[b,c], and Joel A. Swanson[a,b,1]

[a]Biophysics Program and [b]Department of Microbiology and Immunology, University of Michigan, Ann Arbor, MI 48109-5620; and [c]Department of Chemistry and Biochemistry, South Dakota State University, Brookings, SD 57007-0896

Edited by Peter N. Devreotes, The Johns Hopkins University School of Medicine, Baltimore, MD, and approved October 4, 2010 (received for review June 10, 2010)

During Fcγ receptor (FcR)-mediated phagocytosis by macrophages, cytoplasm advances over IgG-coated particles by the sequential ligation of FcR in plasma membranes. If FcR signaling was strictly autonomous, then the signals generated during phagocytosis should be proportional to the number of ligated receptors. By measuring FcR-dependent responses to beads coated with various densities of IgG, this study identified nonlinear signaling that organizes an all or none response during particle ingestion. Phagocytosis of beads with IgG at low density either stalled after making small, actin-rich cups or proceeded to completion at the same rate as phagocytosis of high-density IgG beads. Signals were measured by quantifying the recruitment of YFP-labeled probes to phagocytic cup membranes. Although the magnitude of early signals correlated with IgG density, later signals showed an all or none response, which was regulated by the concentrations of 3′ phosphoinositides in phagocytic cup membranes. Thus, 3′ phosphoinositides, shown previously to be required for phagocytosis, function in a feedback regulatory mechanism affecting late but not early signals. This indicates a mechanism for the coordination of cell movements initiated by receptor signaling.

fluorescence | macrophage | microscopy | phosphatidylinositol 3-kinase | phosphoinositides

In late stages of adaptive immune responses, particles or microbes coated with IgG are efficiently removed by Fcγ receptor (FcR)-mediated phagocytosis into neutrophils and macrophages. FcR binding to IgG triggers a signaling cascade necessary for phagocytosis (1). Ligated FcR on macrophage plasma membranes induces phosphorylation of tyrosines within the immunoreceptor tyrosine-based activation motif of FcR. This leads to recruitment of protein and lipid kinases, such as Syk (2), PI3K (3), and PKCε (4), reorganization of the actin cytoskeleton (5), and increased synthesis of phosphatidylinositol (3,4,5)-trisphosphate (PIP_3), $PI(4,5)P_2$, and diacylglycerol (3, 6). The zipper model of FcR-mediated phagocytosis states that ligands (IgG) and receptors (FcR) interact in an ordered progression as the phagocytic cup advances over the particle, with each ligated receptor generating downstream signals locally and autonomously (7). However, some studies have shown that phagocytosis may be modulated by physical features of particles such as particle stiffness or surface topology (8, 9), which indicate that strictly local signals are insufficient to explain all cellular responses.

If progressively ligated FcR contributes equally and linearly to particle uptake, then the signals generated during phagocytosis should be proportional to the number of ligated receptors. Conversely, if FcR signaling were cooperative, then some or all signals should be subject to feedback regulation related to the number or concentration of activated FcR. To determine whether receptors generate signals independently of each other, we developed a ratiometric fluorescence microscopic method to measure the relationship between IgG density on a particle surface and the magnitude of signaling molecule recruitment to phagocytic cup membranes. We report that the recruitment of early-stage signals correlated with IgG density on beads, consistent with autonomous signaling by FcR. However, later signals showed a different relationship to IgG density. Progression to late stages of signaling and completion of phagocytosis were regulated by 3′ phosphoinositides (3′PI) concentrations in membranes of unclosed phagocytic cups. 3′PI concentration thresholds determined if phagocytic cups stalled or completed phagocytosis, which indicates a mechanism for coordination of signaling by FcR and prompts a revision of the zipper model of phagocytosis.

Results

To vary the numbers of ligated FcR in phagosomes, we prepared 5.6-μm polystyrene beads coated (opsonized) with different densities of Texas Red-conjugated IgG (*SI Appendix*, Fig. S1). The IgG on bead surfaces was measured by fluorescence microscopy and normalized to the lowest density, which generated a phagocytic index higher than 0.5 (B1). Compared with B1, beads with 10-fold higher IgG density (B10) bound to cells more avidly (2.65 ± 0.06 beads/cell for B10 vs. 1.35 ± 0.09 beads/cell for B1) and showed a higher phagocytic index, but their rates of phagosome formation were similar (Fig. 1). At low IgG densities, phagocytosis either stalled after forming shallow cups or proceeded to completion. This indicated that phagocytosis was an all or none response and that FcR signaling was cooperative and subject to feedback regulation.

FcR-generated signals were measured by quantifying the recruitment of YFP-labeled probes to phagosomes containing beads with different densities of surface IgG. We developed a method to quantify the recruitment of YFP chimeras from cytoplasm to phagosomes as a function of IgG density on beads (Fig. 2*A*). Ratiometric fluorescence imaging of macrophages expressing YFP chimeras and free CFP allowed correction for variations in cell thickness (10). Multiplying the CFP image by the average ratio of YFP to CFP fluorescence in the cell (Rc) renormalized the CFP image to the YFP expression level. Subtraction of this YFP path-length image from the original YFP image created an image, Re, whose intensity quantified the specific recruitment of the YFP chimera to subregions of the cell. This method was applied to cells during phagocytosis of beads with varying densities of IgG, which was measured by total fluorescence of Texas Red-IgG. To correct for different sizes of phagocytic cups at various stages of phagosome formation, the average YFP chimera recruitment per pixel was calculated from regions of phagosomes. This allowed comparisons of signals between cups that stalled and cups that completely ingested particles. Images were acquired from cells with similar YFP chimera expression levels to ensure comparable contributions from endogenous signaling molecules. Although this recruitment method could not be applied to fluorescent chimeras of FcR because they are always associated with membranes, it could be used to measure the recruitment of cytoplasmic YFP chimeras essential to phagocytosis.

Early Stages of Signaling Correlate with IgG Density on Beads. Syk recruitment is an early signal generated by ligated FcR (11). Syk-YFP was recruited to phagosomes containing B10 and remained

Author contributions: Y.Z. and J.A.S. designed research; Y.Z. performed research; Y.Z., A.D.H., and J.A.S. analyzed data; and Y.Z. and J.A.S. wrote the paper.

The authors declare no conflict of interest.

This article is a PNAS Direct Submission.

[1]To whom correspondence should be addressed. E-mail: jswan@umich.edu.

This article contains supporting information online at www.pnas.org/lookup/suppl/doi:10.1073/pnas.1008248107/-/DCSupplemental.

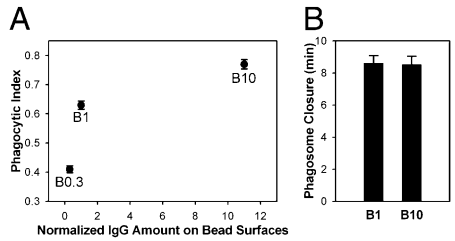

Fig. 1. IgG density on beads controls the frequency but not rate of phagocytosis. (*A*) Phagocytic indexes of B0.3, B1, and B10 were measured from six coverslips. Data represent mean ± SEM. The relationship between ligand density and phagocytic index was nonlinear. (*B*) The rates of phagosome formation were measured as the time from the first movement of cytoplasm to phagosome closure (n = 5).

on phagosomes during internalization (Fig. 2*B*). Low-IgG beads (B1) recruited less Syk-YFP than beads with higher IgG densities (Fig. 2 *C* and *E*). Although total Syk-YFP recruited to the phagosomes increased as cups extended (Fig. 2 *B* and *C*), the average recruitment per pixel remained constant (Fig. 2*E*). Recruitment correlated with ligand density, with some saturation at the highest IgG density (Fig. 2*F*). The recruitment of Syk(R194A)-YFP, containing a point mutation in the SH2 domain that abrogates binding to FcR immunoreceptor tyrosine-based activation motifs (ITAM) (12), was low for both B10 and B1 (Fig. 2 *D* and *F*), indicating the specificity of the recruitment calculation method. Thus, the recruitment of Syk-YFP to phagocytic cup membranes indicated that the magnitude of early FcR signals correlated with ligand density.

To investigate whether signals downstream of Syk are similarly recruited relative to IgG density on beads, we examined the recruitment of YFP-p85, the regulatory domain of type I PI3K, and YFP-actin. p85 binds to Syk directly (13) and indirectly through Gab2 (14) and is recruited to phagosomes early (15). Actin is necessary for phagocytosis (5) and is recruited at the first membrane movement (16). Although B10 recruited more YFP-p85 than B1 (Fig. 2*G*), the difference was only about twofold (Fig. 2*H*), and B10 recruited only 30% more YFP-actin than B1 (Fig. 2 *I* and *J*). These nonlinear signaling responses to 10-fold differences in IgG density suggested differential amplification of FcR signaling, which is inconsistent with a strictly receptor-autonomous signaling mechanism. Because YFP-actin recruitment gave a strong fluorescent signal, we could also quantify YFP-actin in stalled phagocytic cups (covering about one-sixth of the bead surface). The YFP-actin recruited to stalled cups was only slightly lower than that recruited during successful phagocytic events (finished phagosomes) (Fig. 2*J*), indicating that the magnitude of this signal was independent of the outcome of the process.

Later Stages of Signaling Exhibit All or None Behavior. Later stages of signaling showed a binary response related to successful particle ingestion. A YFP chimera of the pleckstrin homology (PH) domain of Abelson tyrosine kinase (YFP-AktPH) was used to localize PIP_3 and $PI(3,4)P_2$, the products of type I PI3K (16). Notably, YFP-AktPH recruitment was similar during phagocytosis of B10 and B1 (Fig. 2 *K* and *L* and *SI Appendix*, Fig. S2 *A* and *B*). BtkPH-YFP, which binds PIP_3 specifically, and YFP-Tapp1PH, which binds $PI(3,4)P_2$ (17), were also recruited to similar levels on B10 and B1 phagosomes (*SI Appendix*, Fig. S3). In contrast, stalled phagocytic cups recruited significantly less YFP-AktPH than did cups that completed phagocytosis, despite similar IgG densities on the beads (Figs. 2*L* and *SI Appendix*, Fig. S2*C*). Thus, 3′PI concentrations were high when phagocytosis could be completed and low when phagocytosis stalled, indicating that PI3K amplification correlated with successful advance of the phagocytic cup.

PKCε-YFP showed a more pronounced threshold response. PKCε recruitment to phagosomes (4) requires binding to diacylglycerol (18). During phagocytosis, diacylglycerol is generated from $PI(4,5)P_2$ by phospholipase C γ-1 (PLCγ1), whose activation requires PIP_3 (19). PKCε-YFP recruitment during phagocytosis increased late during phagosome formation, peaking at the point of phagosome closure (Fig. 3). Remarkably, PKCε-YFP recruitment showed an inverse relationship to IgG density: more chimera was recruited to low-IgG beads than to high-IgG beads (Fig. 3 *D* and *E*). The mechanism of this inverse correlation is unknown. However, the strong signal on low-IgG bead phagosomes exaggerated the difference in signaling between stalled and successful phagocytic cups. PKCε-YFP recruitment was undetectable in stalled cups but was highly amplified on successfully formed phagosomes (Fig. 3 *C* and *E*), indicating that late signal amplification of PKCε-YFP correlated with commitment to phagosome formation.

These measurements indicated that early signaling from FcR was receptor-autonomous and correlated with ligand density, but later signaling showed an all or none response suggestive of feedback regulation. Measurements of the time from the beginning of phagocytic cup formation to the point when recruitment reached half-maximal values showed that the signal sequence of Syk-YFP, YFP-p85, YFP-actin, YFP-AktPH, and then, PKCε-YFP could be detected over the time course of phagocytosis (Fig. 3*F*). Contrary to the model of autonomous signaling by FcR, the ratio of the average maximum recruitment of B1 to that of B10 increased for late signals to greater than one (Fig. 3*G*), indicating aggregate behavior of FcR consistent with signal integration. More significantly, late signals appeared on low-IgG beads only when phagocytosis could be completed. This conditional progression was further evidence of cooperation in FcR signal transduction. It is noteworthy that the late signals AktPH and PKCε reached half-maximal levels (Fig. 3*F*) well before phagosome closure (8 min), indicating that their all or none responses occurred when the phagocytic cup was contiguous with plasma membrane.

3′PI Concentration Thresholds Regulate Commitment to Phagocytosis. The all or none response to low-IgG beads indicated that a concentration threshold regulated the transition to late signals. PI3K regulates contractile activities and membrane fusion necessary for completion of phagocytosis (20, 21). Inhibition of PI3K blocks the activation of Arf1 and Rac2 and the deactivation of Arf6 and Cdc42 during FcR-mediated phagocytosis, which indicates a PIP_3-dependent signal transition governing Arf- and Rho-family GTPase activities. This signal transition is necessary for the phagocytosis of large particles (22, 23). We, therefore, examined the role of PIP_3 in commitment to phagocytosis by modulating the cells' ability to generate PIP_3. Phagocytic indexes were measured for B0.3, B1, and B10 in the presence of inhibitors of PI3K or phosphatase and tensin homolog (PTEN), which dephosphorylates PIP_3 to $PI(4,5)P_2$. The PTEN inhibitor bpv(pic) (24) increased the phagocytic index of both B0.3 and B1, consistent with a positive role for PIP_3 in commitment to phagocytosis (Fig. 4 *A* and *B*). Conversely, the PI3K inhibitor LY294002 inhibited phagocytosis of B1 and B10, and Thrombogenix compound TGX-221, an inhibitor specific for p110β and p110δ isoforms of type I PI3K (25), reduced the phagocytic index of B1 (Fig. 4 *B* and *C*). Furthermore, IgG density on beads correlated inversely with the magnitudes of stimulation by bpv(pic) and inhibition by LY294002, suggesting that the number of ligated FcR affected the cell's ability to exceed a threshold concentration of PIP_3 or a PIP_3-derived 3′PI.

These responses indicated that 3′PI concentrations regulated the transition to late stages of signaling and cellular commitment to phagocytosis. To measure signals regulating commitment, YFP chimera recruitment to stalled cups was compared with chimera recruitment to similarly shaped early cups of finished phagosomes and unfinished cups formed after inhibition of PI3K with LY294002 (3). YFP-actin was recruited to similar levels on stalled cups and early finished cups, and it was present in the unfinished cups of cells inhibited with LY294002 (Fig. 4*D*), indicating that this early signal was independent of PI3K activity and the PIP_3 concentration threshold. Although YFP-AktPH was detectable in stalled cups, its recruitment was significantly

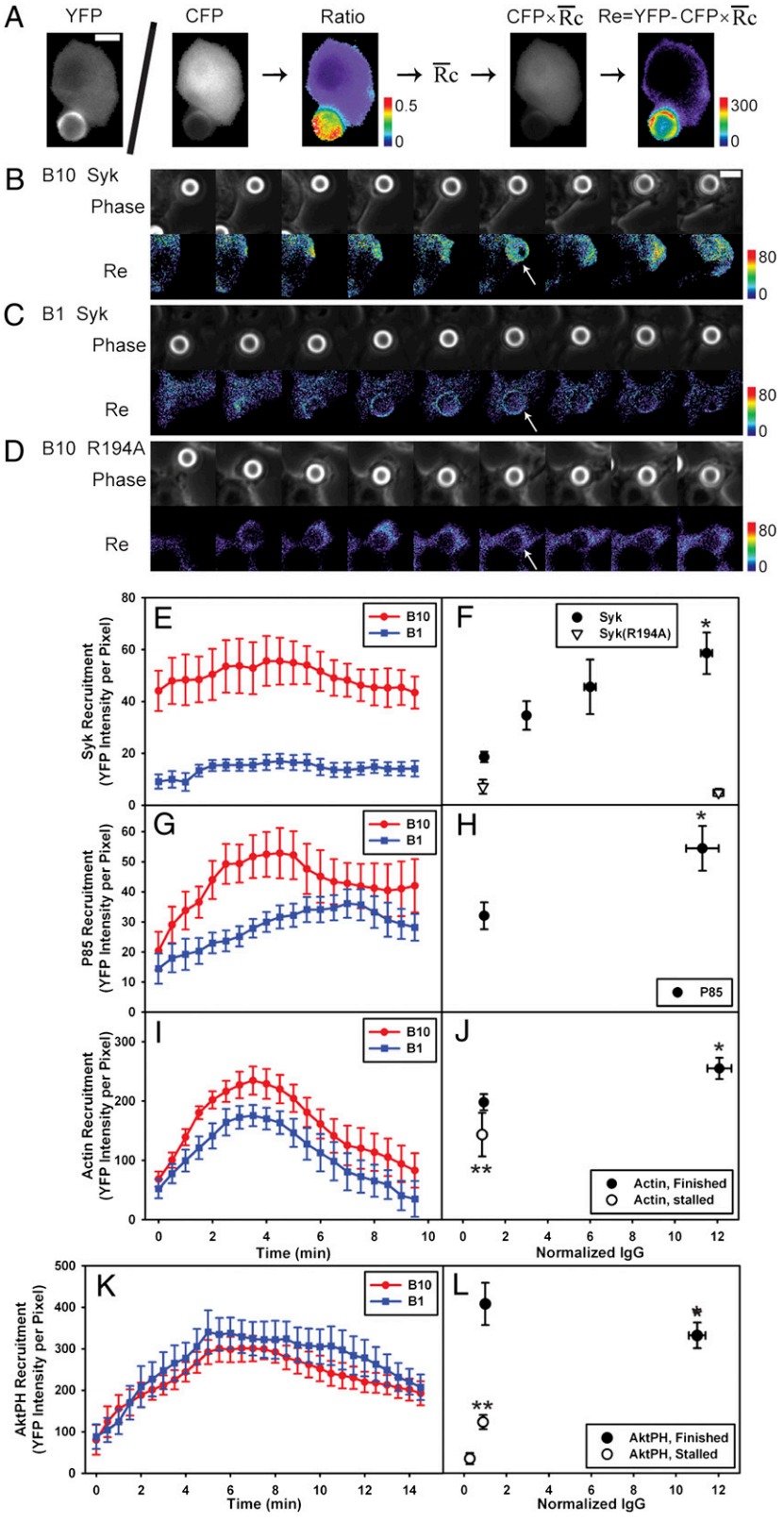

Fig. 2. Quantitation of fluorescent chimera recruitment during phagocytosis. (*A*) In cells expressing YFP chimeras and CFP, the ratio image was calculated by dividing corresponding pixels of the YFP and CFP images. Multiplying the CFP image by the average YFP/CFP ratio in cytosol, $\bar{R}c$(a single number determined for each cell) generated a YFP path-length image representing how that cell's quantity of YFP chimera would appear if it did not contain any localization information. Subtracting this image from the YFP image created a difference image, Re, which represented the quantity of YFP displaced by localization information. (*B–D*) Phase contrast and Re images of Syk-YFP–expressing RAWs internalizing B10 (*B*) and B1 (*C*) and Syk(R194A)-YFP–expressing RAW 264.7 macrophages internalizing B10 (*D*). Arrowheads indicate regions with increased recruitment of Syk-YFP. (Scale bar: 5 μm.) The average recruitments of Syk-YFP (*E*), YFP-p85 (*G*), YFP-actin (*I*), and YFP-AktPH (*K*) per pixel in phagosomes of B10 (red) and B1 (blue) were plotted as a function of time, aligned by the start of membrane movement for phagocytosis. (*F*) The maximum Syk-YFP recruitment averaged from single phagocytic events for B10, B6, B3, and B1 (solid circles; $n = 8$) as well as Syk (R194A)-YFP recruitment for B10 and B1 (open triangles; $n = 4$). B10 phagosomes recruited more YFP-p85 (*H*); $^*P = 0.024$) and YFP-actin (*J*; $^*P = 0.029$) than B1 phagosomes. Stalled phagocytic cups recruited slightly less YFP-actin than did completed phagosomes (open circles; $n = 5$; $^{**}P = 0.129$). (*L*) The maximum YFP-AktPH recruitment during completed phagocytic events (solid circles; $n = 8$) showed no difference between B10 and B1 ($^*P = 0.223$). In contrast, YFP-AktPH recruitment in stalled phagocytic cups (open circle; $n = 5$) increased slightly with ligand density but remained significantly lower than in finished phagosomes ($^{**}P = 0.001$).

less than that in early cups (Fig. 4*E*), indicative of the 3′PI concentration controlling the transition to late signals. This critical PIP_3 concentration difference occurred more than 4 min before phagosome closure (*SI Appendix*, Fig. S4), which further supports the hypothesis that PIP_3 concentration thresholds regulate commitment to phagocytosis. PKCε-YFP was undetectable in stalled cups and cups of LY294002-treated cells (Fig. 4*F*), indicating that its recruitment correlated with commitment to phagocytosis and was responsive to suprathreshold concentrations of 3′PI. Thus, progression to late stages of FcR signaling

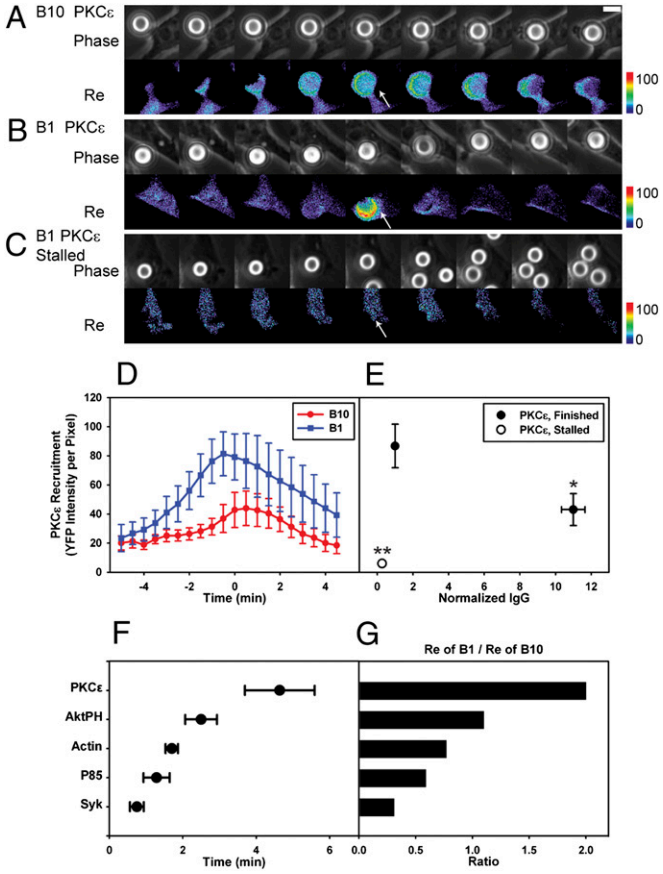

Fig. 3. Late signals correlate inversely with IgG density. (*A*–*C*) Beads coated with higher IgG density recruited less PKCε-YFP to phagosomes during phagocytosis. Time lapse, phase contrast, and Re images of PKCε-YFP–transfected RAWs internalizing B10 (*A*) and B1 (*B*) are shown at 2-min intervals. The arrowheads show that B10 recruited less PKCε-YFP than B1. (Scale bar: 5 μm.) (*C*) Stalled phagocytic cups did not recruit PKCε-YFP. (*D*) The average recruitment of PKCε-YFP per pixel in phagosomes aligned by the timing of phagosome closure ($n = 8$). (*E*) The maximum PKCε-YFP recruitment of completed phagocytic events (solid circles) showed that B1 recruited more PKCε-YFP than B10 did ($*P = 0.034$). In addition, PKCε-YFP recruitment to stalled phagocytic cups (open circles; $n = 10$) was significantly lower than in finished phagosomes ($**P < 0.0001$). (*F*) Times for half-maximal recruitment during phagocytosis of B10. Phagocytosis of B1 showed similar half-maximal recruitment times with slightly longer values for Syk-YFP (1.8 ± 0.37 min) and YPF-p85 (2.9 ± 0.6 min). All values show mean ± SEM. (*G*) Ratios of maximal YFP chimera recruitment to B1 vs. B10.

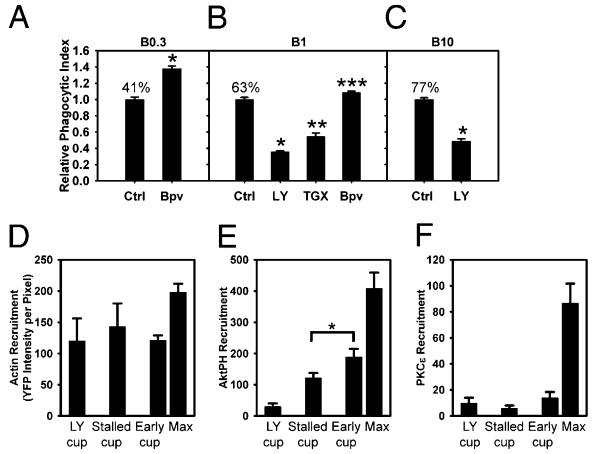

Fig. 4. 3′PIs regulate commitment to phagocytosis with different effects on early and late signals. (*A*) Effect of Bpv(pic) on the phagocytic index of B0.3 ($n = 6$; $*P < 0.0001$). (*B*) Effects of inhibitors on the phagocytic indexes of B1. Bpv(pic) increased phagocytic index, whereas LY294002 and TGX-221 decreased phagocytic indexes ($n = 6$; $*P < 0.01$, $**P < 0.001$, $***P < 0.0001$). (*C*) Effect of LY294002 on the phagocytic index of B10 ($n = 6$; $*P < 0.0001$). Percentages indicate actual phagocytic indexes. (*D*–*F*) Recruitment of YFP-actin (*D*), YFP-AktPH (*E*), and PKCε-YFP (*F*) to cups in LY294002-treated cells (LY cups) and stalled cups and early (early cup) and maximal values (max) for successfully formed B1 phagosomes. Early cups were similar in size and shape to stalled cups, using frames from early time points of successful phagocytic events. YFP-AktPH recruitment to early cups was greater than recruitment to stalled cups ($n = 5$; $*P = 0.045$). LY294002 did not inhibit the recruitment of YFP-actin (*D*; $n = 3$) but inhibited the recruitment of YFP-AktPH (*E*) and PKCε-YFP (*F*; $n = 5$).

and completion of phagocytosis require a minimum concentration of 3′PIs in the membranes of unclosed phagocytic cups.

Discussion

Using a quantitative method to evaluate the relationship between ligand density on particles and the signals generated by FcR, this study identified significantly different properties of early and late signals for phagocytosis. At low IgG densities, FcR activated some but not all signals necessary for phagocytosis. This is contrary to the segmental responses predicted by the zipper model and indicates that complete signaling for phagocytosis requires the coordination of multiple receptors. Moreover, a 3′PI concentration threshold controls progression to late signals and cellular commitment to phagocytosis, which indicates that a zipper-like mechanism is modulated by feedback regulation based on the magnitude of the stimulus.

Three lines of evidence indicated coordination of FcR signaling controlling commitment to phagocytosis. First, low IgG density on beads reduced the fraction of bound particles ingested but not the rate of phagosome formation. Second, during phagocytosis of low IgG-density beads, stalled phagocytic cups accumulated low levels of 3′PI and negligible levels of YFP-PKCε, but fully formed phagocytic cups recruited as much or more of those molecules than did phagosomes with high IgG-density beads. Third, commitment to phagocytosis was regulated by concentrations of PIP_3 or PIP_3-derived 3′PIs in phagocytic cups, indicating that 3′PI concentration thresholds control a transition from local, autonomous responses to the coordinated movements of phagosome formation (Fig. 5). Threshold-dependent FcR signaling was most strikingly evident on low-IgG beads, which always recruited similar amounts of YFP-actin (early signal), but recruited high concentrations of YFP-PKCε (late signal) when phagocytosis was completed and negligible concentrations when phagocytosis stalled.

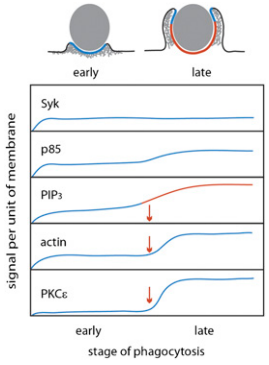

Fig. 5. A 3′PI concentration threshold regulates commitment to late stages of signaling. Signaling during internalization by phagocytosis was divided into early- and late-stage signals, depending on whether they appeared before or after PIP_3 generation. Recruitment of the late-signal PKCε required 3′PIs to exceed a concentration threshold, whereas early-stage signals, such as Syk, P85, and actin, did not. However, optimal recruitment of actin and p85 may require suprathreshold 3′PIs.

The patterns of YFP chimera association with phagosomes indicated both the sequence of signaling as well as differential regulation of the related signals. The sequence of early to late signals was evident in the YFP chimera association kinetics (Fig. 3*F*). Although all chimera recruitment peaked at or before phagosome closure, the patterns of dissociation varied considerably. Syk-YFP remained associated with the phagosomes, but other chimeras dissociated from the phagosomes. YFP-actin dissociated dramatically, consistent with its patterns of advance over particles (16) and the role of the signal transition in actin depolymerization (23). YFP-p85 and YFP-AktPH both were lost from phagosomes after closure. The loss of YFP-AktPH may indicate the activities of phospholipases or other phospholipid kinases affecting the levels of PIP_3 or $PI(3,4)P_2$. Finally, the differential magnitudes of PKCε-YFP recruitment to B1 and B10 indicated a feedback regulation in which IgG density modulates the magnitude of late signals during successful phagosome formation. Such signal suppression at high IgG densities could buffer macrophage effector mechanisms.

Other studies have identified effects of ligand density on signaling for phagocytosis. Dale et al. (26) showed that IgG density can regulate particle binding. We observed a similar relationship. Sil et al. (27) developed soluble IgE ligands with different molecular spacing and showed effects of ligand geometry on Fcε receptor signaling in mast cells. Ligand geometry and concentration showed differential effects on various receptor signals. Some geometry-dependent signals from Fcε receptors were more sensitive to PLC inhibitors than to PI3K inhibitors. The present study is distinct from those earlier studies in its identification of the correlation between the timing of signals generated by FcR and their relative dependence on IgG density and 3′PIs.

It is possible that the dramatically different responses of cells to B1 particles (stalling vs. complete ingestion) were regulated by small differences in the number of FcR ligated by the beads, differences sufficient to determine sub- vs. suprathreshold levels of 3′ PIs. The recruitment method did not allow us to measure recruitment of FcR directly into forming phagosomes, because YFP-FcR chimeras are integral membrane proteins. Consequently, we could not directly measure the number of FcR activated by individual particles. Instead, we used the recruitment of Syk-YFP, which binds to FcR directly, to represent the earliest measureable signal downstream of receptor binding.

The timing of YFP-AktPH recruitment was consistent with a causative role for 3′PI concentrations in commitment to phagocytosis. Earlier studies showed that PIP_3 concentrations are elevated in cup membranes before phagosome closure (15, 28). Locally elevated PIP_3 concentrations in plasma membranes have also been described for macropinocytic cups (29). Additionally, measurements of the time, relative to phagosome closure, when YFP-AktPH recruitment exceeded the threshold showed that the concentrations of 3′PIs necessary for commitment to phagosome formation were reached several minutes before cup closure (*SI Appendix*, Fig. S4). Thus, the suprathreshold concentrations of PIP_3 occur in unclosed cups, consistent with a role for 3′PI concentrations regulating commitment to phagocytosis.

How might 3′PI concentrations regulate commitment? Phagocytic cup membranes may create thresholds for signal transitions through low-affinity 3′PI binding domains in regulatory enzymes (30–33). For example, suprathreshold concentrations of PIP_3 in phagocytic cups could be required to activate PLCγ1 for synthesis of diacylglycerol and recruitment of PKCε. Moreover, the signal transition, in which early GTPases are deactivated and late GTPases are activated, is regulated by PI3K and is necessary for completion of phagocytosis (22, 23). The 3′PI concentration threshold could regulate activation of a 3′PI-dependent guanine nucleotide exchange factor (GEF) or GTPase-accelerating protein (GAP), which is rate-limiting for the signal transition.

Why should opsonin density be decoded in this manner? A threshold-based transition to late signals may modulate cellular responses to smaller particles or soluble immune complexes, thereby controlling damage to tissues by inflammatory responses. Moreover, subthreshold responses by FcR could be an entirely distinct class of FcR signaling that pertains to small particles. For example, subthreshold FcR signaling could organize ARF1- and PKCε-independent actin-based movements, which may allow macrophages either to ingest small particles without activating microbicidal chemistries or to explore IgG-coated surfaces without attempting phagocytosis.

How might this feedback regulation be reconciled with the zipper model? Threshold-based transitions to all or none responses are more consistent with the trigger model for phagocytosis, which was originally proposed as an alternative to the zipper model (7). We propose that, although FcR activates small segments of plasma membrane, additional regulation organizes the movements that follow. Accordingly, early signals generated by FcR may be autonomous and directly responsive to IgG binding, but additional signals must be coordinated over multiple FcR for commitment to formation of phagosomes around large particles. The distribution and density of IgG on a particle surface could localize the PI3K amplification mechanism, thereby restricting signaling to a zipper-like movement over an opsonized surface.

Materials and Methods

Material and DNA Constructs. Streptavidin-coated, 5.6-μm diameter polystyrene beads were purchased from Bangs Laboratories. Texas Red-conjugated rabbit antibodies (IgG) to streptavidin were from Abcam. Plasmids encoding monomeric CFP and Citrine (YFP), a YFP variant, were used for all constructs (34). Constructs of YFP chimeras of actin, AktPH, Tapp1PH, and p85 were described previously (15, 16). Plasmids encoding Syk and PKCε were gifts from Robert Geahlen (Purdue University, West Lafayette, IN) and Peter Lipp (Saarland University, Homburg, Germany), respectively, and were subcloned into mCitrine-N1 vectors (Clontech). The mutant construct Syk(R194A)-YFP was made from Syk-YFP by the QuikChange Site-Directed Mutagenesis Kit (Stratagene).

Microsphere Opsonization and Phagocytic Index Assay. Ten-microliter beads were opsonized with different amounts of IgG in 200 μL PBS with 1% BSA, incubated at 37 °C for 30 min, and washed three times with 500 μL PBS with 1% BSA to remove excess IgG before adding to cells for imaging. To measure the phagocytic index, RAW264.7 cells were plated 18 h before inhibitor treatment (5×10^4 cells per 13-mm coverslip). Thirty minutes after treatment with 50 μM LY294002, 100 nM TGX-221, or 200 nM bpv(pic) (EMD Chemicals), beads opsonized with Texas Red-IgG were added, and the macrophages were allowed to internalize the particles for 30 min at 37 °C. Cells were then rinsed with PBS and fixed. Beads that were not completely internalized were marked with Alexa 488-conjugated goat anti-rabbit IgG (Invitrogen). The phagocytic index was counted for at least 50 macrophages per coverslip and measured as the percent of bound particles successfully internalized by macrophages.

Microscopy. Cell culture and transfection of the macrophage-like cell line RAW264.7 (American Type Culture Collection) for fluorescence microscopy were described previously (22). Time-lapse images of phase-contrast, CFP, and YFP were acquired at 30-s intervals using a microscope described previously (22). YFP images were taken using 100-ms exposure or normalized to 100 ms if other exposure times were used. The ligand (Texas Red-IgG) densities of the internalized beads were measured from images in the Texas Red Isothiocyanate (TRITC) channel (Excitation 555 ± 14 nm; Emission 605 ± 20 nm). Rates of phagocytosis were obtained from video sequences of CFP fluorescence obtained during particle ingestion. Phagocytosis was not synchronized artificially; instead, the beginning of phagocytosis was identified by the first increase in CFP fluorescence near a bound particle, and the complete internalization of the particle was indicated by displacement of cytoplasmic CFP.

Because the results of the recruitment calculation and bead opsonization measurement were in units of YFP and TRITC intensities, respectively, it was necessary to calibrate the illumination intensity of the xenon lamp as the bulb aged. The calibration images of a mixture of green and red fluorescent beads (M7901 Component B; Invitrogen) were taken in YFP and TRITC channels. The average intensities of beads were calculated in both channels and divided by the values acquired at the time of bulb installation to generate a microscope intensity calibration factor (MICF). Both the recruitment calculation and measurement of bead opsonization were divided by the MICF to normalize illumination intensities of the microscope.

Image Analysis by Recruitment Calculation. The recruitment calculation was performed by journals developed in Metamorph (Molecular Devices). The bias

and shading corrections of YFP and CFP images, described previously (35), generated YFPb and CFPb images, respectively. A ratio image (R) was calculated by dividing the YFPb image by the corresponding CFPb image and multiplying by 1,000 to avoid truncation of significant digits in the integral math of Metamorph.

To quantify the recruitment of YFP chimeras to phagosomes, a 5.6-μm circular region was created in the phase-contrast image and positioned over the internalized beads during phagocytosis by the tracking algorithm TRACOBJ in Metamorph (10). The average intensities in the bead regions transferred to YFPb and CFPb, excluding the noncell portion, were recorded as YFPp and CFPp, respectively. For YFP-AktPH, which distributes similarly to free CFP in resting cells, the average values of cell regions in R images were recorded as $\bar{R}c$. For YFP chimeras of p85, Syk, actin, and PKCε, which do not localize to nuclei as much as free CFP, the nuclear regions of cells were eliminated in YFPb, CFPb, and R images by an additional mask created by a manual threshold in R images. The average value of the cell region excluding the nucleus in R images was recorded as $\bar{R}c$. The recruitment of YFP chimeras of signaling molecules to phagosomes (Re) was calculated by Eq. **1**. The product of CFPp and $\bar{R}c$/1,000 represented how that quantity of YFP would appear if there were no specific recruitment; its difference from YFPp was proportional to the number of YFP chimeras recruited to phagosome.

$$\mathrm{Re} = \frac{\left(YFPp - CFPp \times \bar{R}c/1,000\right)}{MICF} \quad [1]$$

In control experiments, we measured YFP recruitment during ingestion of opsonized beads by RAW264.7 macrophages transfected with YFP and CFP and found that this method returned average values of recruitment per pixel of 6.4 ± 2.1 in phagosomal areas, which represent the systematic error of this imaging method and was subtracted as baseline in subsequent recruitment measurements.

Statistical Analysis. To compare means of data from different groups, a Student *t* test was performed using the data analysis tool in Excel (Microsoft).

ACKNOWLEDGMENTS. This work was supported by National Institutes of Health Grants AI35950 and AI64668 (to J.A.S.).

1. Swanson JA, Hoppe AD (2004) The coordination of signaling during Fc receptor-mediated phagocytosis. *J Leukoc Biol* 76:1093–1103.
2. Nimmerjahn F, Ravetch JV (2006) Fcgamma receptors: Old friends and new family members. *Immunity* 24:19–28.
3. Araki N, Johnson MT, Swanson JA (1996) A role for phosphoinositide 3-kinase in the completion of macropinocytosis and phagocytosis by macrophages. *J Cell Biol* 135: 1249–1260.
4. Larsen EC, et al. (2002) A role for PKC-ε in Fc gammaR-mediated phagocytosis by RAW 264.7 cells. *J Cell Biol* 159:939–944.
5. May RC, Machesky LM (2001) Phagocytosis and the actin cytoskeleton. *J Cell Sci* 114: 1061–1077.
6. Botelho RJ, et al. (2000) Localized biphasic changes in phosphatidylinositol-4,5-bisphosphate at sites of phagocytosis. *J Cell Biol* 151:1353–1368.
7. Griffin FM, Jr, Griffin JA, Leider JE, Silverstein SC (1975) Studies on the mechanism of phagocytosis. I. Requirements for circumferential attachment of particle-bound ligands to specific receptors on the macrophage plasma membrane. *J Exp Med* 142:1263–1282.
8. Beningo KA, Wang Y-L (2002) Fc-receptor-mediated phagocytosis is regulated by mechanical properties of the target. *J Cell Sci* 115:849–856.
9. Champion JA, Mitragotri S (2006) Role of target geometry in phagocytosis. *Proc Natl Acad Sci USA* 103:4930–4934.
10. Henry RM, Hoppe AD, Joshi N, Swanson JA (2004) The uniformity of phagosome maturation in macrophages. *J Cell Biol* 164:185–194.
11. Sada K, Takano T, Yanagi S, Yamamura H (2001) Structure and function of Syk protein-tyrosine kinase. *J Biochem* 130:177–186.
12. Mócsai A, et al. (2006) Integrin signaling in neutrophils and macrophages uses adaptors containing immunoreceptor tyrosine-based activation motifs. *Nat Immunol* 7:1326–1333.
13. Moon KD, et al. (2005) Molecular basis for a direct interaction between the Syk protein-tyrosine kinase and phosphoinositide 3-kinase. *J Biol Chem* 280:1543–1551.
14. Gu H, Botelho RJ, Yu M, Grinstein S, Neel BG (2003) Critical role for scaffolding adapter Gab2 in Fc gamma R-mediated phagocytosis. *J Cell Biol* 161:1151–1161.
15. Kamen LA, Levinsohn J, Swanson JA (2007) Differential association of phosphatidylinositol 3-kinase, SHIP-1, and PTEN with forming phagosomes. *Mol Biol Cell* 18:2463–2472.
16. Hoppe AD, Swanson JA (2004) Cdc42, Rac1, and Rac2 display distinct patterns of activation during phagocytosis. *Mol Biol Cell* 15:3509–3519.
17. Varnai P, Thyagarajan B, Rohacs T, Balla T (2006) Rapidly inducible changes in phosphatidylinositol 4,5-bisphosphate levels influence multiple regulatory functions of the lipid in intact living cells. *J Cell Biol* 175:377–382.
18. Cheeseman KL, et al. (2006) Targeting of protein kinase C-epsilon during Fcgamma receptor-dependent phagocytosis requires the epsilonC1B domain and phospholipase C-gamma1. *Mol Biol Cell* 17:799–813.
19. Bae YS, et al. (1998) Activation of phospholipase C-gamma by phosphatidylinositol 3,4,5-trisphosphate. *J Biol Chem* 273:4465–4469.
20. Swanson JA, et al. (1999) A contractile activity that closes phagosomes in macrophages. *J Cell Sci* 112:307–316.
21. Cox D, Tseng C-C, Bjekic G, Greenberg S (1999) A requirement for phosphatidylinositol 3-kinase in pseudopod extension. *J Biol Chem* 274:1240–1247.
22. Beemiller P, Hoppe AD, Swanson JA (2006) A phosphatidylinositol-3-kinase-dependent signal transition regulates ARF1 and ARF6 during Fcgamma receptor-mediated phagocytosis. *PLoS Biol* 4:e162.
23. Beemiller P, et al. (2010) A Cdc42 activation cycle coordinated by PI 3-kinase during Fc receptor-mediated phagocytosis. *Mol Biol Cell* 21:470–480.
24. Schmid AC, Byrne RD, Vilar R, Woscholski R (2004) Bisperoxovanadium compounds are potent PTEN inhibitors. *FEBS Lett* 566:35–38.
25. Chaussade C, et al. (2007) Evidence for functional redundancy of class IA PI3K isoforms in insulin signalling. *Biochem J* 404:449–458.
26. Dale BM, Traum D, Erdjument-Bromage H, Tempst P, Greenberg S (2009) Phagocytosis in macrophages lacking Cbl reveals an unsuspected role for Fc gamma receptor signaling and actin assembly in target binding. *J Immunol* 182:5654–5662.
27. Sil D, Lee JB, Luo D, Holowka D, Baird B (2007) Trivalent ligands with rigid DNA spacers reveal structural requirements for IgE receptor signaling in RBL mast cells. *ACS Chem Biol* 2:674–684.
28. Marshall JG, et al. (2001) Restricted accumulation of phosphatidylinositol 3-kinase products in a plasmalemmal subdomain during Fc gamma receptor-mediated phagocytosis. *J Cell Biol* 153:1369–1380.
29. Yoshida S, Hoppe AD, Araki N, Swanson JA (2009) Sequential signaling in plasma-membrane domains during macropinosome formation in macrophages. *J Cell Sci* 122: 3250–3261.
30. Swanson JA (2008) Shaping cups into phagosomes and macropinosomes. *Nat Rev Mol Cell Biol* 9:639–649.
31. Falasca M, et al. (1998) Activation of phospholipase C gamma by PI 3-kinase-induced PH domain-mediated membrane targeting. *EMBO J* 17:414–422.
32. Klarlund JK, et al. (1998) Regulation of GRP1-catalyzed ADP ribosylation factor guanine nucleotide exchange by phosphatidylinositol 3,4,5-trisphosphate. *J Biol Chem* 273:1859–1862.
33. Krugmann S, Andrews S, Stephens L, Hawkins PT (2006) ARAP3 is essential for formation of lamellipodia after growth factor stimulation. *J Cell Sci* 119:425–432.
34. Zacharias DA, Violin JD, Newton AC, Tsien RY (2002) Partitioning of lipid-modified monomeric GFPs into membrane microdomains of live cells. *Science* 296:913–916.
35. Hoppe A, Christensen KA, Swanson JA (2002) Fluorescence resonance energy transfer-based stoichiometry in living cells. *Biophys J* 83:3652–3664.